Original Article | Technology, Experiment, and Physics

https://doi.org/10.3348/kjr.2018.19.6.1161
pISSN 1229-6929 · eISSN 2005-8330
Korean J Radiol 2018;19(6):1161-1171

Korean Journal of Radiology
KJR

Diffusion Tensor-Derived Properties of Benign Oligemia, True "at Risk" Penumbra, and Infarct Core during the First Three Hours of Stroke Onset: A Rat Model

Fang-Ying Chiu, PhD[1*], Duen-Pang Kuo, PhD[2*], Yung-Chieh Chen, PhD, MD[3, 4], Yu-Chieh Kao, PhD[4], Hsiao-Wen Chung, PhD[5], Cheng-Yu Chen, MD[3, 4, 6-8]

[1]Department of Medical Imaging and Radiological Sciences, College of Medicine, I-Shou University, Kaohsiung 82445, Taiwan; [2]Department of Radiology, Taoyuan Armed Forces General Hospital, Taoyuan 32551, Taiwan; [3]Department of Medical Imaging, Taipei Medical University Hospital, Taipei Medical University, Taipei 11031, Taiwan; [4]Translational Imaging Research Center, College of Medicine, Taipei Medical University, Taipei 11031, Taiwan; [5]Graduate Institute of Biomedical Electrics and Bioinformatics, National Taiwan University, Taipei 10617, Taiwan; [6]Department of Radiology, School of Medicine, College of Medicine, Taipei Medical University, Taipei 11031, Taiwan; [7]Department of Radiology, Tri-Service General Hospital, Taipei 11490, Taiwan; [8]Department of Radiology, National Defense Medical Center, Taipei 11490, Taiwan

Objective: The aim of this study was to investigate diffusion tensor (DT) imaging-derived properties of benign oligemia, true "at risk" penumbra (TP), and the infarct core (IC) during the first 3 hours of stroke onset.

Materials and Methods: The study was approved by the local animal care and use committee. DT imaging data were obtained from 14 rats after permanent middle cerebral artery occlusion (pMCAO) using a 7T magnetic resonance scanner (Bruker) in room air. Relative cerebral blood flow and apparent diffusion coefficient (ADC) maps were generated to define oligemia, TP, IC, and normal tissue (NT) every 30 minutes up to 3 hours. Relative fractional anisotropy (rFA), pure anisotropy (rq), diffusion magnitude (rL), ADC (rADC), axial diffusivity (rAD), and radial diffusivity (rRD) values were derived by comparison with the contralateral normal brain.

Results: The mean volume of oligemia was 24.7 ± 14.1 mm^3, that of TP was 81.3 ± 62.6 mm^3, and that of IC was 123.0 ± 85.2 mm^3 at 30 minutes after pMCAO. rFA showed an initial paradoxical 10% increase in IC and TP, and declined afterward. The rq, rL, rADC, rAD, and rRD showed an initial discrepant decrease in IC (from -24% to -36%) as compared with TP (from -7% to -13%). Significant differences ($p < 0.05$) in metrics, except rFA, were found between tissue subtypes in the first 2.5 hours. The rq demonstrated the best overall performance in discriminating TP from IC (accuracy = 92.6%, area under curve = 0.93) and the optimal cutoff value was -33.90%. The metric values for oligemia and NT remained similar at all time points.

Conclusion: Benign oligemia is small and remains microstructurally normal under pMCAO. TP and IC show a distinct evolution of DT-derived properties within the first 3 hours of stroke onset, and are thus potentially useful in predicting the fate of ischemic brain.

Keywords: *Diffusion tensor imaging; True penumbra; Infarct core; Benign oligemia; Pure anisotropy; Diffusion magnitude*

Received February 14, 2018; accepted after revision April 27, 2018.
This study was supported by the Ministry of Science and Technology, Taiwan, grants serial 105-2221-E-038 -007 -MY3.
Dr. Cheng-Yu Chen received government grant support from the Ministry of Science and Technology, Taiwan, for work related to hyperacute stroke.

*These authors contributed equally to this work.

Corresponding author: Cheng-Yu Chen, MD, Department of Medical Imaging, Taipei Medical University Hospital, Taipei Medical University, No.252, Wu Xing street, SinYi Distric, Taipei 11031, Taiwan.
• Tel: (8862) 27372181 • Fax: (8862) 2378-0943 • E-mail: sandy0932@gmail.com

INTRODUCTION

Ischemic penumbra (IP) is defined as non-functional but living brain tissue at risk of infarct following large vessel occlusion (1). This critical area of the ischemic zone, as opposed to the dead infarct core (IC), has long been the therapeutic target since the early trials with intravenous thrombolytic therapies (2, 3). It remains controversial whether imaging-defined IP should also include benign oligemia-which is hypoperfused, functionally normal, and not at risk of infarct-as the target of intervention (4). In the era of intra-arterial thrombectomy with a longer therapeutic time window, the need for improved discrimination of oligemia from true "at-risk" penumbra (TP) by non-invasive imaging methods has increased as the outcome of clinical stroke trials can be quantitatively measured (5).

With non-invasive magnetic resonance imaging (MRI), IP can be assessed by the mismatch between the diffusion-weighted imaging hyperintensity (IC) and the perfusion-weighted imaging (PWI) deficit (reduced cerebral blood flow) (6). While this method is clinically practical, there are inherent conceptual and technical flaws in perfusion measures (7). First, perfusion imaging does not reflect metabolic states of IP, which evolve dynamically. Second, the technical assumption for perfusion imaging, particularly deconvolution-based approaches, requires correct arterial input function and flows, without significant delay or dispersion. Furthermore, perfusion measures such as mean transit time and time to peak have not been standardized, and can easily be affected by delayed collaterals and flow dispersion. Therefore, rather than pursuing a mismatch concept, a direct measurement of microstructure injury of the brain to differentiate ischemic tissue such as IC, penumbra at risk, and benign oligemia is desirable.

Diffusion tensor imaging (DTI) is a relatively new technique for non-invasive delineation of cerebral micro-structural changes. It measures tensor metrics, including eigenvalue magnitudes and anisotropy (8). Recent investigations have shown the feasibility of DTI in assessing the microstructure of the ischemic brain tissue (9, 10). DTI metrics, such as fractional anisotropy (FA), can be employed as surrogate markers in studying cell membrane integrity over time after injuries (7). Furthermore, a recent study reported the utility of DTI in determining the onset time of ischemic stroke by hours in a rat model with hyperoxygenation treatment (11). The purpose of this study was to investigate diffusion tensor (DT)-derived properties of benign oligemia, TP, and the IC during the first 3 hours of stroke onset under room air.

MATERIALS AND METHODS

Animal Preparations

This study was approved by the local institutional animal care and use committee. Fourteen male Sprague-Dawley rats (weight, 270–350 g; Taipei Medical University Animal Center, Taiwan) were used in this study. They were housed in a humidity- and temperature-controlled environment and placed under a 12:12-hour light:dark cycle, with free access to sterile food and water. All rats underwent permanent left middle cerebral artery occlusion (pMCAO) via an intra-luminal suture method based on the modified Zea Longa approach.

MRI

All animal imaging sessions were performed using a 7T scanner (PharmaScan 70/16; Bruker Biospin, Ettlingen, Germany). The rats were maintained under anesthesia using 1.5–2% isoflurane and kept under regular room air during image acquisition. Rectal temperature was maintained at 37°C using a warm water bath with continuous circulation through a water-bath temperature controller set outside the magnet. DTI was performed with six non-collinear diffusion-encoding gradients with a b factor of 1200 s/mm^2 plus one b = 0 s/mm^2. Multi-shot echo-planar imaging (repetition time [TR] = 3000 ms, echo time [TE] = 37 ms, number of excitations = 6) with navigator-echo correction technique was used as the signal readout module. The longitudinal evolutions of DTI metrics of the rat brain were obtained by performing six sequential DTI scans for every rat, with the first scan performed at 30 minutes post-pMCAO, and then every 30 minutes up to 3 hours. PWI was performed at 30 minutes post-pMCAO using a dynamic susceptibility contrast (DSC) technique. A series of gradient-echo echo-planar, coronal images with TR/TE of 1000/20 ms and 300 repetitions were acquired. A bolus of the susceptibility contrast agent gadolinium-diethylenetriamine penta-acetic acid (0.25 mmol/kg; Magnevist, Bayer Schering Pharma, Berlin, Germany) was injected manually via the rat tail vein about 30 seconds after the start of image acquisition. The perfusion deficits were measured only once to calculate the perfusion/diffusion mismatch at 30 minutes and at the five follow-up time points. All image matrices were zero-filled to 128 x 128 for further analyses.

Korean Journal of Radiology
KJR

Data Analysis

Calculation of Relative Cerebral Blood Flow (rCBF) and DTI Metrics

The rCBF and DTI metrics were calculated and compared with those of the contralateral normal brain using in-house algorithms in MATLAB (MathWorks, Natick, MA, USA). For rCBF, the concentration-time curves were first obtained from signal-time curves of DSC perfusion imaging, with the recirculation effect being minimized via gamma-variate fitting (12, 13). The relative cerebral blood volume (rCBV) and relative mean transit time (rMTT) were then determined by the integral and the normalized first moment of the gamma variate fitting, respectively, as follows (14, 15):

$$\mathrm{rCBV} = \int \Delta_2(t)dt$$

$$\mathrm{rMTT} = \frac{\int t \times \Delta_2(t)dt}{\int \Delta R_2(t)dt}$$

where ΔR_2 is the change in transverse relaxation rate and *t* is the time after bolus arrival. Using the central volume principle, rCBF is derived as the quotient of CBV divided by MTT (16). For DTI metrics, the eigenvalues (λ_1, λ_2, λ_3) of each image voxel were computed, and then applied to derive the mean diffusivity (MD), FA, pure anisotropy (q), diffusion magnitude (L), axial diffusivity (AD), and radial diffusivity (RD) (10, 17-20) (Fig. 1). The equations are illustrated as follows:

$$\mathrm{MD} = \mathrm{D} = \frac{\lambda_1 + \lambda_2 + \lambda_3}{3},$$

$$AD = \lambda_1,\ RD = \frac{\lambda_2 + \lambda_3}{2}$$

$$q = \sqrt{(\lambda_1 - D)^2 + (\lambda_2 - D)^2 + (\lambda_3 - D)^2},\ L = \sqrt{\lambda_1^2 + \lambda_2^2 + \lambda_3^2}$$

$$FA = \sqrt{\frac{3}{2}}\frac{q}{L}$$

Delineation of TP, IC, and Oligemia

Infarct core was defined as a hypodense area in the apparent diffusion coefficient (ADC) map at 30 minutes post-pMCAO (Fig. 2A) while IC_{3h} was the same growing hypodense area at 3 hours (Fig. 2B). Perfusion deficit was first defined at 30 minutes post-pMCAO (Fig. 2C). Regions ipsilateral to pMCAO with reduction in rCBF below 63% of the contralateral homologous brain were considered as CBF deficits (21). The rCBF map was then co-registered to the ADC maps of each follow-up time point to delineate the perfusion-diffusion mismatch, with the threshold of abnormal ADC change set at 70% of the normal contralateral cerebral hemisphere (19, 22). Based on the results, IC was defined as regions showing rCBF

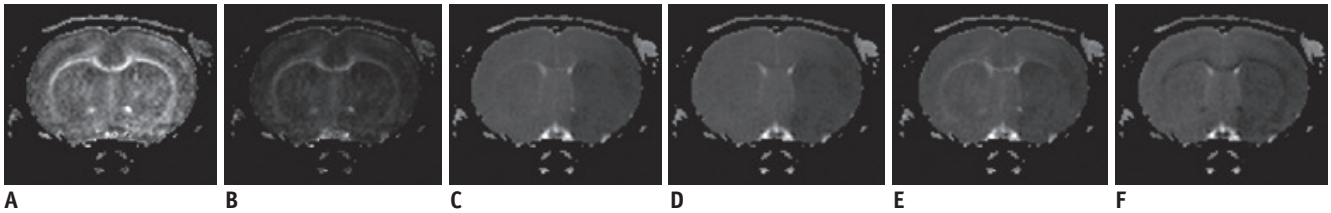

Fig. 1. Maps of DTI metrics measured at 30 minutes post pMCAO.
Note relative hypointensity changes within hemisphere ipsilateral to pMCAO on maps of q **(B)**, L **(C)**, MD **(D)**, AD **(E)**, and RD **(F)**, with exception of FA **(A)** which shows symmetrical signal intensity. AD = axial diffusivity, DTI = diffusion tensor imaging, FA = fractional anisotropy, L = diffusion magnitude, MD = mean diffusivity, pMCAO = permanent middle cerebral artery occlusion, q = pure anisotropy, RD = radial diffusivity

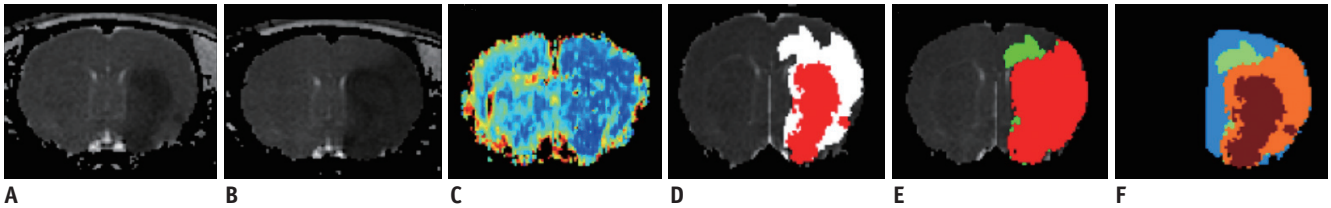

Fig. 2. Definitions of oligemia, TP, IC, and final infarct (IC_{3h}) in pMCAO rat.
IC was defined as hypodense area in apparent diffusion coefficient map at 30 minutes post pMCAO **(A)** while IC_{3h} was same growing hypodense area at 3 hours **(B)**. Perfusion deficit at 30 minutes post pMCAO is shown in **(C)**. Perfusion-diffusion mismatch is illustrated in **(D)** where red indicates IC and white perfusion deficit (including oligemia and TP) at 30 minutes post pMCAO. Oligemia (green in **E, F**) was defined as $CBF_{0.5h}$ - IC_{3h} mismatch. TP (orange in **F**) was difference between IC_{3h} and IC at 30 minutes. CBF = cerebral blood flow, IC = infarct core, TP = true penumbra

values < 63% and ADC < 70%, while TP and oligemic tissues were delineated together as regions showing rCBF values < 63% and ADC > 70% (Fig. 2D). Regions without CBF deficit within the ipsilateral brain were defined as normal tissue (NT). To differentiate benign oligemia from TP, we compared the initial extent of CBF deficit at 30 minutes post-pMCAO ($CBF_{0.5h}$) with the region of IC at 3 hours (IC_{3h}) (Fig. 2E), which was previously shown to be equivalent to the final infarct area at 24 hours post-pMCAO (23) (Fig. 2D). Based on the notion that TP will irreversibly progress to IC in the absence of timely reperfusion while oligemic tissue will not, the region of oligemia was hence extracted by excluding the region of IC_{3h} from that of $CBF_{0.5h}$ after image co-registration, i.e., $CBF_{0.5h}$–IC_{3h} mismatch (Fig. 2F). This method was repeated at each following time point to obtain the respective regions of IC, TP, and oligemic tissue in all rats. Finally, once the regions of interest (ROIs) of TP, IC, NT, and oligemia were depicted by the mismatches, the relative DTI metrics, including relative MD (rMD), rAD, rRD, rFA, rL, and rq values, were derived and expressed as percentages of the corresponding values in the homologous contralateral brain as follows: $rX = (X_{ipsilateral} - X_{contralateral}) / X_{contralateral}$, where X indicates the value of the particular index. In addition, all ROIs were transposed onto DT maps at each time point for testing regional differences and time-courses analyses.

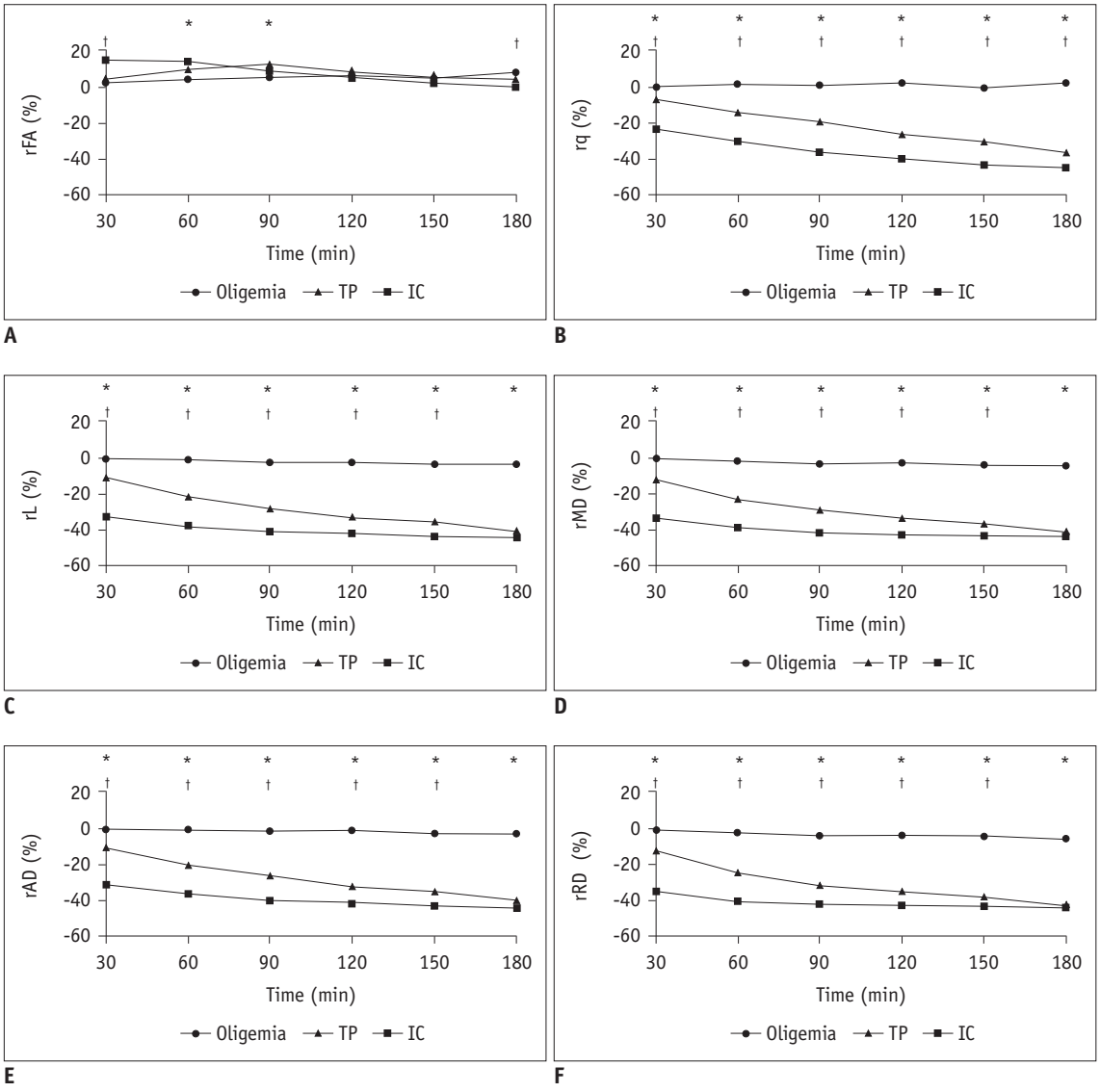

Fig. 3. Temporal evolution of DTI metrics within 3 hours post-pMCAO in oligemia, TP, and IC.
In particular, significant differences ($p < 0.05$) in DTI metrics between oligemia, TP, and IC, including rFA **(A)**, rq **(B)**, rL **(C)**, rMD **(D)**, rAD **(E)**, and rRD **(F)** are highlighted across time points. *TP vs. oligemia, †TP vs. IC. rAD = relative AD, rFA = relative FA, rL = relative L, rMD = relative MD, rq = relative q, rRD = relative RD

Korean Journal of Radiology
KJR

Statistical Analysis

Statistical tests were performed using SPSS® for Windows software (Version 18.0; SPSS Inc., Chicago, IL, USA) to determine whether the pMCAO DTI metrics can be used to discriminate TP from IC, oligemia, and NT, regardless of the time effect. ANOVA with post hoc analysis was employed to evaluate whether the means of DTI metrics were significantly different between the TP, IC, oligemia, and NT regions at each imaging time point. Receiver operating characteristic (ROC) curve analyses were performed to determine the discriminative capability of the diffusion metrics to differentiate NT, oligemia, TP, and IC at each time point. A p value < 0.05 was considered statistically significant.

RESULTS

Temporal Evolutions of DTI Metrics among Tissue Types

Figure 1 illustrates the maps of DTI metrics at 30 minutes post-pMCAO. The q, L, MD, AD, and RD maps demonstrate initial hypointensity changes in the ischemic areas while the FA map exhibits symmetrical signal intensity. Figure 3 shows the temporal evolutions of DTI metrics in IC, TP, and oligemia from 30 minutes post pMCAO to 3 hours. All the metrics among different tissue types showed a trend of decline with time, with the exception of rFA, which displayed a paradoxical 10% increase in IC and TP in the first 60 minutes, followed by a subtle steady decrease to close to zero (i.e., nearly identical to the contralateral

Table 1. Measurements of Relative DTI Metrics in IC, TP, Oligemia and NT as Compared to Contralateral Homologous Normal Brain at Each Time Point (All Numbers in Percentages)

DTI metrics*	30 Min	60 Min	90 Min	120 Min	150 Min	180 Min
IC						
rFA	14.17 ± 1.49	13.40 ± 2.19	8.66 ± 2.23	5.04 ± 2.15	1.62 ± 2.16	-0.90 ± 1.92
rq	-24.08 ± 1.14	-30.46 ± 1.44	-37.03 ± 1.20	-40.41 ± 1.60	-43.64 ± 1.72	-45.35 ± 1.51
rL	-33.21 ± 0.72	-38.45 ± 1.15	-41.44 ± 1.38	-42.66 ± 1.32	-43.78 ± 1.40	-44.44 ± 1.17
rMD	-33.97 ± 0.73	-39.20 ± 1.20	-41.88 ± 1.44	-42.93 ± 1.36	-43.94 ± 1.43	-44.46 ± 1.19
rAD	-31.68 ± 0.73	-37.10 ± 1.11	-40.76 ± 1.27	-42.41 ± 1.29	-43.88 ± 1.39	-44.82 ± 1.15
rRD	-35.80 ± 0.80	-40.88 ± 1.34	-42.78 ± 1.62	-43.34 ± 1.50	-44.01 ± 1.56	-44.17 ± 1.32
TP						
rFA	4.58 ± 1.28	10.24 ± 1.90	12.32 ± 1.74	8.77 ± 1.42	6.72 ± 1.49	4.73 ± 1.64
rq	-6.94 ± 1.39	-14.20 ± 1.73	-19.33 ± 2.10	-26.35 ± 2.03	-30.60 ± 2.83	-36.98 ± 2.72
rL	-11.37 ± 1.24	-22.36 ± 1.50	-28.43 ± 2.04	-33.00 ± 1.97	-36.26 ± 2.24	-40.79 ± 1.83
rMD	-11.88 ± 1.31	-23.17 ± 1.54	-29.45 ± 2.02	-33.71 ± 1.96	-36.95 ± 2.18	-41.37 ± 1.71
rAD	-10.69 ± 1.18	-20.95 ± 1.45	-26.82 ± 2.01	-31.81 ± 1.99	-35.25 ± 2.35	-40.20 ± 1.97
rRD	-12.88 ± 1.47	-24.97 ± 1.72	-31.68 ± 2.07	-35.34 ± 1.95	-38.40 ± 2.06	-42.42 ± 1.50
Oligemia						
rFA	1.62 ± 1.06	3.77 ± 1.66	4.79 ± 2.05	6.13 ± 1.89	4.47 ± 1.58	7.56 ± 2.39
rq	-0.59 ± 1.23	1.31 ± 1.70	0.76 ± 1.80	1.67 ± 1.78	-1.26 ± 1.58	1.50 ± 1.99
rL	-1.25 ± 0.63	-1.70 ± 0.66	-3.32 ± 0.81	-3.04 ± 0.84	-4.35 ± 0.86	-4.58 ± 0.86
rMD	-1.32 ± 0.62	-2.01 ± 0.70	-3.70 ± 0.90	-3.45 ± 0.90	-4.62 ± 0.89	-5.11 ± 0.94
rAD	-1.13 ± 0.68	-1.10 ± 0.62	-2.52 ± 0.68	-2.13 ± 0.84	-3.75 ± 0.92	-3.35 ± 0.84
rRD	-1.46 ± 0.67	-2.76 ± 0.96	-4.60 ± 1.20	-4.45 ± 1.11	-5.22 ± 0.99	-6.48 ± 1.24
NT						
rFA	3.81 ± 0.78	4.26 ± 0.87	4.88 ± 1.22	5.47 ± 1.16	4.45 ± 1.03	9.66 ± 0.97
rq	-1.37 ± 0.62	-1.57 ± 0.95	-1.59 ± 1.06	-1.91 ± 0.88	-4.20 ± 0.88	2.53 ± 0.74
rL	-2.60 ± 0.77	-4.05 ± 0.83	-3.98 ± 0.91	-4.51 ± 0.93	-5.83 ± 1.04	-1.37 ± 1.27
rMD	-2.76 ± 0.81	-4.33 ± 0.85	-4.30 ± 0.96	-4.84 ± 1.00	-6.08 ± 1.11	-1.84 ± 1.34
rAD	-2.41 ± 0.70	-3.63 ± 0.80	-3.54 ± 0.83	-4.14 ± 0.82	-5.68 ± 0.96	-0.87 ± 1.08
rRD	-3.04 ± 0.92	-4.89 ± 0.92	-4.92 ± 1.12	-5.40 ± 1.17	-6.37 ± 1.26	-2.59 ± 1.57

*DTI metrics were defined as rX = ($X_{ipsilateral}$ - $X_{contralateral}$) / $X_{contralateral}$, where X indicates value of indices (mean ± standard error of the mean). DTI = diffusion tensor imaging, IC = infarct core, NT = normal tissue, rAD = relative axial diffusivity, rFA = relative fractional anisotropy, rL = relative diffusion magnitude, rMD = relative mean diffusivity, rq = relative pure anisotropy, rRD = relative radial diffusivity, TP = true penumbra

normal tissue [NT]). The rL and rq that compose the rFA exhibited reductions in both TP and IC during the period of pMCAO (Fig. 3A-C, Table 1). The rq showed changes from -6.94% at 30 minutes to -36.98% at 3 hours in TP, and from -24.08% at 30 minutes to -45.35% at 3 hours in IC (Table 1). The rL showed a relatively larger reduction as compared to rq in both TP and IC within 3 hours (Table 1). rMD in $TP_{0.5\text{-}3.0h}$ showed a monotonic decrease from a reduction of -11.88% at 30 minutes to -41.37% at 3 hours (Table 1), while in $IC_{0.5\text{-}3.0h}$, rMD had a reduction of 33.97% at 30 minutes and remained steady (Fig. 3D, Table 1). The evolutions of rq, rAD, and rRD (Fig. 3E, F) followed the profile of rMD. Significant differences ($p < 0.05$) in all DTI metrics except rFA were found between TP and oligemia, and between TP and IC before 2.5 hours (Fig. 3). The rFA showed significant differences between TP and oligemia at 60 minutes ($p = 0.016$) and 90 minutes ($p = 0.010$). All DTI metrics for oligemia and NT remained steady with no significant difference across different time points (NT not shown in Fig. 3).

Topographic Distributions of the IC, TP, and Oligemia as Ischemia Progressed in the First 3 Hours

Figure 4 shows the representative topographic maps of the IC, TP, and oligemia in each slice at different time points. Both oligemia and TP are small in areas at the margin of a larger IC. Oligemia was smaller than TP and located at the outermost margin of TP. As time evolved, TP showed a progressive decrease in volume within the first 2.5 hours and ultimately progressed to IC at 3 hours. Infarct volumes of all rats (n = 14) at the 30-minute and 3-hour time points are plotted in Figure 5 shows the mean volumes of $IC_{0.5h}$ (123.0 ± 85.2 mm^3), $IC_{3.0h}$ (204.3 ± 104.2 mm^3), oligemia (24.7 ± 14.1 mm^3), and TP (81.3 ± 62.6 mm^3).

Discrimination of TP from Oligemia, IC, and NT by DTI Metrics

Significant differences ($p < 0.05$) in rq, rL, rMD, rAD,

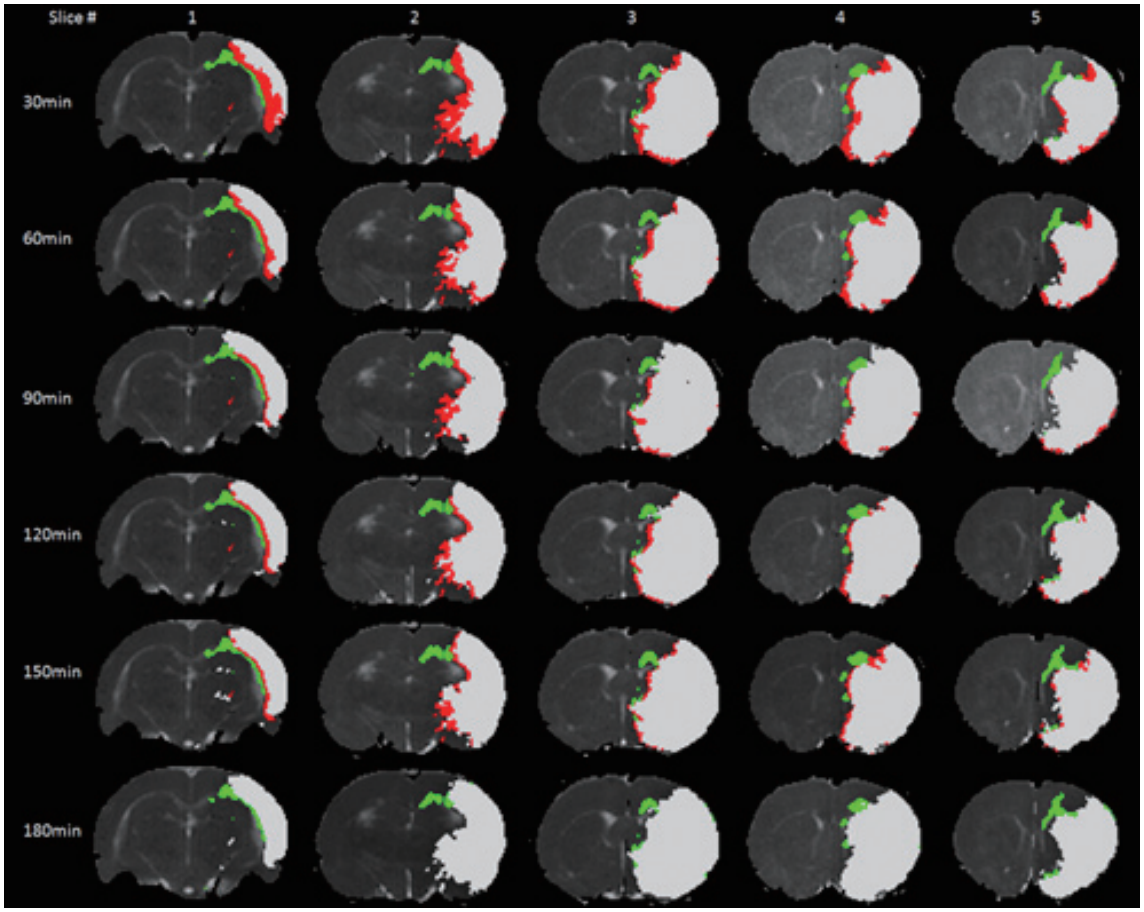

Fig. 4. Topographic distributions of IC, TP, and oligemia with ischemia progression. NT is displayed in grayscale, core in white, TP in red, and oligemia in green. As time evolved, TP gradually merged into IC and disappeared, while oligemia persisted during first 3 hours post pMCAO. NT = normal tissue

Korean Journal of Radiology
KJR

and rRD values were found between tissue subtypes at time points before 150 minutes (Fig. 3). ROC analysis for discriminating between oligemia and TP, as well as between TP and IC, showed good performance for all metrics, except rFA. Representative ROC curves and the best cutoff values for discriminating tissue subtypes at 90 minutes post-pMCAO are shown in Figure 6 and Table 2, respectively (see Appendix for ROC curves at 30, 60, and 90 minutes; Supplementary Tables 1-3, Supplementary Figs. 1-3 in the online-only Data Supplement), and show that all metrics except rFA had excellent performance in discriminating TP from IC, as well as in discriminating TP from oligemia (average accuracy > 90%). The rq had the best overall performance in discriminating TP from IC (accuracy = 92.6%, area under curve = 0.93) and the optimal cutoff value was -33.90% (Table 2). For discrimination of TP from oligemia, the rL, rMD, rAD, and rRD values all exhibited accuracies larger than 97.8%. Oligemia and NT were indiscriminative at all time points.

DISCUSSION

In this study, we characterized the temporal evolution of DTI metrics within different brain tissue subtypes, such as IC, TP, oligemia, and NT during the first 3 hours after pMCAO. Our findings were three-fold: First, the volume of oligemia was small. Its tensor properties were similar to those of normal brain tissue, and completely different

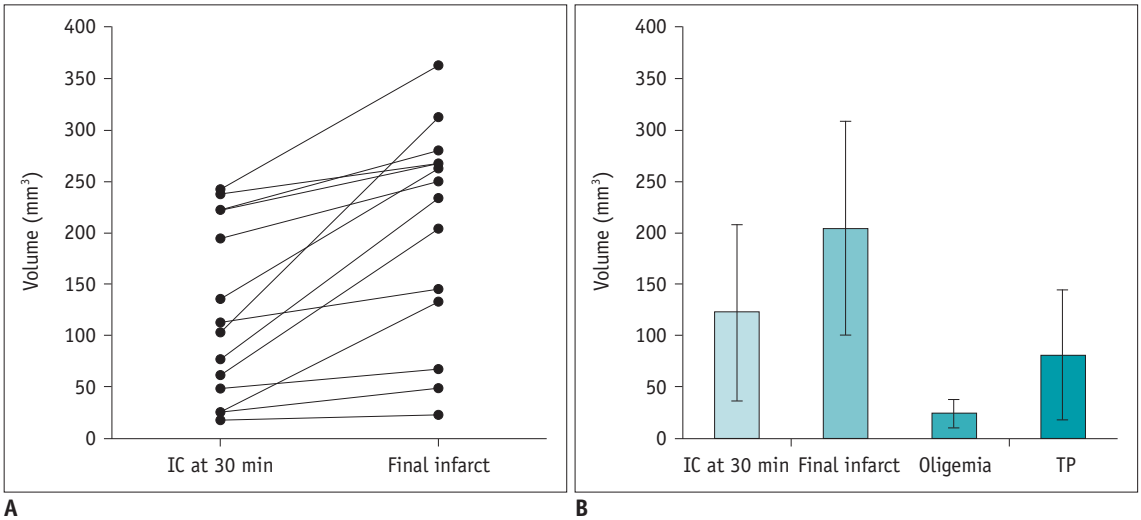

Fig. 5. Volumes of IC at 30 minutes and final infarct, oligemia, and TP at 3 hours.
A. Comparison of infarct sizes (mm^3) between 0.5 hours and 3 hours in all rats (n = 14). **B.** Mean volumes of IC at 30 minutes, final infarct, TP, and oligemia at 3 hours. Data presented as mean ± standard deviation.

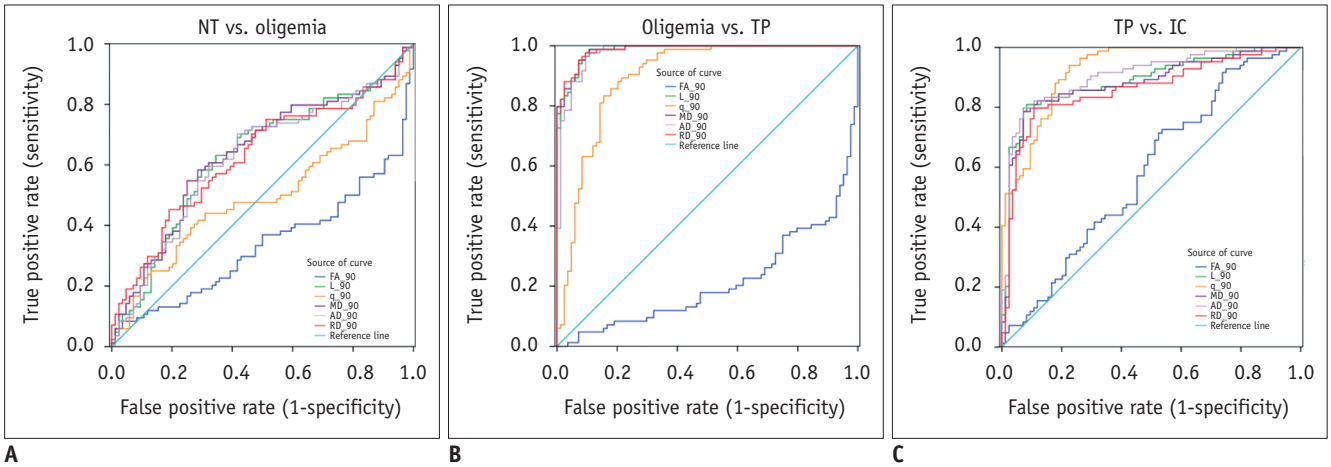

Fig. 6. Imaging A-C encompasses three different receiver operating characteristic curves but similar comparisons.
Receiver operating characteristic curves for discriminating NT from oligemia **(A)**, oligemia from TP **(B)**, and TP from IC **(C)**, using diffusion metrics at 90 minutes post-pMCAO.

Table 2. Discrimination Performance Based on DTI Metrics at 90 Minutes Post Permanent Middle Cerebral Artery Occlusion

DTI metrics	Accuracy (%)	Best Cut Off (%)	Sensitivity	Specificity	Area Under Curve
NT vs. oligemia					
rFA	33.40	18.03	0.08	0.96	0.33
rq	49.40	0.74	0.39	0.74	0.49
rL	62.80	-3.10	0.58	0.70	0.63
rMD	63.50	-2.99	0.55	0.75	0.64
rAD	62.00	-4.31	0.70	0.58	0.62
rRD	62.60	-2.35	0.45	0.81	0.63
Oligemia vs. TP					
rFA	21.30	112.43	0.00	1.00	0.21
rq	89.60	-10.39	0.83	0.85	0.90
rL	98.50	-16.92	0.99	0.89	0.99
rMD	98.60	-14.08	0.95	0.93	0.99
rAD	97.80	-14.47	0.96	0.91	0.98
rRD	98.70	-16.57	0.95	0.93	0.99
TP vs. IC					
rFA	58.30	6.79	0.71	0.48	0.58
rq	92.60	-33.90	0.94	0.77	0.93
rL	88.80	-37.28	0.81	0.92	0.89
rMD	88.10	-37.06	0.79	0.93	0.88
rAD	90.60	-35.08	0.80	0.93	0.91
rRD	85.90	-39.32	0.80	0.89	0.86

from those of TP and IC. Second, rFA, the most frequently investigated DTI parameter, exhibited a paradoxical increase in TP and IC during the first hour post-pMCAO, and did not appear to be useful in discriminating ischemic tissue subtypes. Third, the evolution of DTI metrics such as rL, rq, rMD, rAD, and rRD in TP was distinct from that in IC and oligemia until 2.5 hours post-pMCAO. After 2.5 hours, the features became insignificant as the TP progressed to IC. These findings are in line with those of a previous study that used a histology-validated stroke model (23).

Kuo et al. (11) used DTI metrics to characterize IP in a normobaric hyperoxygenation stroke model up to 6.5 hours post-pMCAO. The prolonged IP was successfully differentiated from that of IC by the selected tensor metrics. In our study, not only was the utility of DTI metrics in delineating IP validated, but DTI was also shown to further discriminate IP into benign oligemia and TP, thus allowing for full visualization and assessment of the four tissue subtypes, which is in alignment with the "four tissue compartments concept" proposed by Lee et al. (24). Our current study was performed in regular room air instead of normobaric hyperoxia, and thus allowed us to assess the natural time course of penumbra development without manual intervention in temporal dynamics. Additionally, we adopted the infarct volume at 3 hours post-pMCAO as the cut-off point to define the final infarct volume. This design was based on an earlier animal study by Meng et al. (23), which demonstrated that the infarct volume at 3 hours post-stroke was highly correlated with that at 24 hours through histological validation. Thus, we were able to investigate the evolution of benign oligemia and true at-risk penumbra using DTI metrics every 30 minutes, for 6 time points, within the first 3 hours after pMCAO.

Among the various DT parameters, FA has been examined extensively in both human stroke studies and animal models as a potential imaging biomarker (8, 9, 11, 17, 25-40). However, the evolution of FA during hyperacute stroke has not yielded consistent results, with studies reporting both increases and decreases in FA during the initial hours, as well as findings showing no significant changes at all (16, 25-33). Nevertheless, our results are in agreement with those of a recent study by Kuo et al. (11) in that rFA was paradoxically elevated in IC during the first hour post-pMCAO, regardless of its cortical or subcortical involvement. As rFA is proportional to the ratio of rq to rL, the increase in rFA was due to a larger reduction in rL value relative to a smaller reduction in rq. During the first 60 minutes post-pMCAO, a larger reduction in rL values (from -33.21% to -38.45%) relative to a smaller reduction in rq (from -24.08% to -30.46%) was observed in the IC (Table 1), resulting in

Korean Journal of Radiology
KJR

an approximate 10% increase in rFA. After 60 minutes, the reduction of rq became greater with time than rL, leading to a slight decrease below the baseline in rFA at 3 hours. The subsequent progressive decline in rFA at 3 hours post-pMCAO was also observed previously in animal studies (30). Intriguingly, this overall trend may also be observed in TP but not in oligemia, which resembles its NT counterpart. Finally, based on our ROC analyses, the discriminative power of FA in separating TP from IC and benign oligemia was poor overall, unlike the other DTI metrics studied which showed high accuracy in the differentiation of tissue subtypes.

Pathophysiologically, ischemic stroke is a complex neuronal condition that involves transmembrane ionic disequilibrium, oxidative stress, axonal disruption, and neuronal swelling, ultimately leading to irreversible neuronal damage and cell death (34). In particular, intracellular glucose and oxygen deprivation because of Na+/K+ ATPase ion pump dysfunction may induce osmotic shift, thus causing cytotoxic edema and neurite beading-processes that can be detected and quantitatively measured via DTI (25, 35, 36). Previous studies have shown that DTI metrics can reflect regional differences in pathophysiologic response towards neuronal ischemia during hyperacute stroke (11). For example, elevations of FA within the region of IC in both grey and white matter have been considered early indicators of ischemic microstructural injury during hyperacute stroke, including axonal damage, disruption of membrane permeability, myelin fiber swelling, and cytotoxic edema with increased tortuosity of the axoplasmic environment (13, 28, 37-39). The subsequent reductions in FA during acute and subacute stages have been found to be linked to progressive loss of neuronal integrity (39). While the current study demonstrated an initial 10% increase in FA within the IC and TP, this was actually a result of anisotropy/magnitude ratio dependence (40). In our analysis, q and L appear independently to be more informative than FA in characterizing tissue diffusion changes in hyperacute stroke (11). As to the other DT metrics, the monotonic decreases in MD, AD, and RD in TP were similar to those of q and L, indicative of continuous degradation of cell membrane integrity, leading to loss of directional diffusivity. Conversely, as benign oligemia is characterized by regional neuronal metabolic and electrical disruption in the absence of significant neuron damage, the presentation of relatively stable DTI metrics, coupled with decreased CBF and sustained ADC value, likely reflects protective compensatory neurovascular autoregulation that helps maintain ionic homeostasis while ameliorating the development of cytotoxic edema (41-44).

There are several limitations in our study. First, our methodology for delineating the region of oligemia in the rat stroke model was based on a modified perfusion-diffusion mismatch approach that has inherent limitations due to the deconvolution model employed, thus potentially leading to over-estimation of the size of IP and oligemia. However, CBF values obtained from perfusion MRI have previously demonstrated excellent correlation with those generated from quantitative positron-emission tomography (PET) in terms of penumbra detection in stroke studies (45). Thus, MR-derived perfusion parameters remain valuable in assessing tissue perfusion. Future studies that involve penumbra or oligemia assessment should ideally incorporate quantitative metabolic measures that reflect true underlying metabolic condition, preferably with PET imaging (21). Second, the regions of oligemia we obtained were relatively small as compared to the regions of TP and IC (Fig. 5); therefore, the limited image pixels may lead to increased vulnerability in terms of metric calculation and accuracy of analyses. Third, the correlation between microstructural injury and DTI metric alternations is still unknown. Therefore, region-wise histopathological correlation may be a desirable next step to provide further proof of the value of DTI as a useful imaging biomarker for stroke studies.

In conclusion, our results suggest that DTI holds promise in discriminating oligemia from TP and IC in the first 3 hours of stroke through direct assessment of the microstructural changes over time. Oligemia is small in size in hyperacute stroke, and thus, it could be of minimal concern when stroke trials require quantitative measurements of IP.

Supplementary Materials

The online-only Data Supplement is available with this article at https://doi.org/10.3348/kjr.2018.19.6.1161.

REFERENCES

1. Hossmann KA, Heiss WD, Bewermeyer H, Mies G. EEG frequency analysis in the course of acute ischemic stroke. *Neurosurg Rev* 1980;3:31-36
2. Hacke W, Kaste M, Bluhmki E, Brozman M, Dávalos A, Guidetti D, et al.; ECASS Investigators. Thrombolysis with alteplase 3 to 4.5 hours after acute ischemic stroke. *N Engl J Med*

2008;359:1317-1329
3. Albers GW, Thijs VN, Wechsler L, Kemp S, Schlaug G, Skalabrin E, et al.; DEFUSE Investigators. Magnetic resonance imaging profiles predict clinical response to early reperfusion: the diffusion and perfusion imaging evaluation for understanding stroke evolution (DEFUSE) study. *Ann Neurol* 2006;60:508-517
4. Heiss WD. Ischemic penumbra: evidence from functional imaging in man. *J Cereb Blood Flow Metab* 2000;20:1276-1293
5. Albers GW, Lansberg MG, Kemp S, Tsai JP, Lavori P, Christensen S, et al. A multicenter randomized controlled trial of endovascular therapy following imaging evaluation for ischemic stroke (DEFUSE 3). *Int J Stroke* 2017;12:896-905
6. Butcher KS, Parsons M, MacGregor L, Barber PA, Chalk J, Bladin C, et al.; EPITHET Investigators. Refining the perfusion-diffusion mismatch hypothesis. *Stroke* 2005;36:1153-1159
7. Goyal M, Menon BK, Derdeyn CP. Perfusion imaging in acute ischemic stroke: let us improve the science before changing clinical practice. *Radiology* 2013;266:16-21
8. Sakai K, Yamada K, Nagakane Y, Mori S, Nakagawa M, Nishimura T. Diffusion tensor imaging may help the determination of time at onset in cerebral ischaemia. *J Neurol Neurosurg Psychiatry* 2009;80:986-990
9. Puig J, Blasco G, Daunis-I-Estadella J, Thomalla G, Castellanos M, Soria G, et al. Increased corticospinal tract fractional anisotropy can discriminate stroke onset within the first 4.5 hours. *Stroke* 2013;44:1162-1165
10. Chiang T, Messing RO, Chou WH. Mouse model of middle cerebral artery occlusion. *J Vis Exp* 2011;(48). pii: 2761
11. Kuo DP, Lu CF, Liou M, Chen YC, Chung HW, Chen CY. Differentiation of the infarct core from ischemic penumbra within the first 4.5 hours, using diffusion tensor imaging-derived metrics: a rat model. *Korean J Radiol* 2017;18:269-278
12. Ostergaard L, Weisskoff RM, Chesler DA, Gyldensted C, Rosen BR. High resolution measurement of cerebral blood flow using intravascular tracer bolus passages. Part I: mathematical approach and statistical analysis. *Magn Reson Med* 1996;36:715-725
13. Lee EK, Choi SH, Yun TJ, Kang KM, Kim TM, Lee SH, et al. Prediction of response to concurrent chemoradiotherapy with temozolomide in glioblastoma: application of immediate post-operative dynamic susceptibility contrast and diffusion-weighted MR imaging. *Korean J Radiol* 2015;16:1341-1348
14. Calamante F, Gadian DG, Connelly A. Quantification of perfusion using bolus tracking magnetic resonance imaging in stroke: assumptions, limitations, and potential implications for clinical use. *Stroke* 2002;33:1146-1151
15. Wu O, Østergaard L, Weisskoff RM, Benner T, Rosen BR, Sorensen AG. Tracer arrival timing-insensitive technique for estimating flow in MR perfusion-weighted imaging using singular value decomposition with a block-circulant deconvolution matrix. *Magn Reson Med* 2003;50:164-174
16. Sakai K, Yamada K, Oouchi H, Nishimura T. Numerical simulation model of hyperacute/acute stage white matter infarction. *Magn Reson Med Sci* 2008;7:187-194
17. Shereen A, Nemkul N, Yang D, Adhami F, Dunn RS, Hazen ML, et al. Ex vivo diffusion tensor imaging and neuropathological correlation in a murine model of hypoxia-ischemia-induced thrombotic stroke. *J Cereb Blood Flow Metab* 2011;31:1155-1169
18. Bråtane BT, Walvick RP, Corot C, Lancelot E, Fisher M. Characterization of gadolinium-based dynamic susceptibility contrast perfusion measurements in permanent and transient MCAO models with volumetric based validation by CASL. *J Cereb Blood Flow Metab* 2010;30:336-342
19. Henninger N, Bouley J, Nelligan JM, Sicard KM, Fisher M. Normobaric hyperoxia delays perfusion/diffusion mismatch evolution, reduces infarct volume, and differentially affects neuronal cell death pathways after suture middle cerebral artery occlusion in rats. *J Cereb Blood Flow Metab* 2007;27:1632-1642
20. Yao X, Yu T, Liang B, Xia T, Huang Q, Zhuang S. Effect of increasing diffusion gradient direction number on diffusion tensor imaging fiber tracking in the human brain. *Korean J Radiol* 2015;16:410-418
21. Lythgoe MF, Thomas DL, Calamante F, Pell GS, King MD, Busza AL, et al. Acute changes in MRI diffusion, perfusion, T(1), and T(2) in a rat model of oligemia produced by partial occlusion of the middle cerebral artery. *Magn Reson Med* 2000;44:706-712
22. Shen Q, Meng X, Fisher M, Sotak CH, Duong TQ. Pixel-by-pixel spatiotemporal progression of focal ischemia derived using quantitative perfusion and diffusion imaging. *J Cereb Blood Flow Metab* 2003;23:1479-1488
23. Meng X, Fisher M, Shen Q, Sotak CH, Duong TQ. Characterizing the diffusion/perfusion mismatch in experimental focal cerebral ischemia. *Ann Neurol* 2004;55:207-212
24. Lee DH, Kang DW, Ahn JS, Choi CG, Kim SJ, Suh DC. Imaging of the ischemic penumbra in acute stroke. *Korean J Radiol* 2005;6:64-74
25. Liu Y, D'Arceuil HE, Westmoreland S, He J, Duggan M, Gonzalez RG, et al. Serial diffusion tensor MRI after transient and permanent cerebral ischemia in nonhuman primates. *Stroke* 2007;38:138-145
26. Morita N, Harada M, Uno M, Furutani K, Nishitani H. Change of diffusion anisotropy in patients with acute cerebral infarction using statistical parametric analysis. *Radiat Med* 2006;24:253-259
27. Tamura H, Kurihara N, Machida Y, Nishino A, Shimosegawa E. How does water diffusion in human white matter change following ischemic stroke? *Magn Reson Med Sci* 2009;8:121-134
28. Bhagat YA, Hussain MS, Stobbe RW, Butcher KS, Emery DJ, Shuaib A, et al. Elevations of diffusion anisotropy are associated with hyper-acute stroke: a serial imaging study. *Magn Reson Imaging* 2008;26:683-693
29. Ozsunar Y, Koseoglu K, Huisman TA, Koroshetz W, Sorensen

AG. MRI measurements of water diffusion: impact of region of interest selection on ischemic quantification. *Eur J Radiol* 2004;51:195-201
30. Carano RA, Li F, Irie K, Helmer KG, Silva MD, Fisher M, et al. Multispectral analysis of the temporal evolution of cerebral ischemia in the rat brain. *J Magn Reson Imaging* 2000;12:842-858
31. Harris AD, Pereira RS, Mitchell JR, Hill MD, Sevick RJ, Frayne R. A comparison of images generated from diffusion-weighted and diffusion-tensor imaging data in hyper-acute stroke. *J Magn Reson Imaging* 2004;20:193-200
32. Sorensen AG, Wu O, Copen WA, Davis TL, Gonzalez RG, Koroshetz WJ, et al. Human acute cerebral ischemia: detection of changes in water diffusion anisotropy by using MR imaging. *Radiology* 1999;212:785-792
33. Zelaya F, Flood N, Chalk JB, Wang D, Doddrell DM, Strugnell W, et al. An evaluation of the time dependence of the anisotropy of the water diffusion tensor in acute human ischemia. *Magn Reson Imaging* 1999;17:331-348
34. Deb P, Sharma S, Hassan KM. Pathophysiologic mechanisms of acute ischemic stroke: an overview with emphasis on therapeutic significance beyond thrombolysis. *Pathophysiology* 2010;17:197-218
35. Pitkonen M, Abo-Ramadan U, Marinkovic I, Pedrono E, Hasan KM, Strbian D, et al. Long-term evolution of diffusion tensor indices after temporary experimental ischemic stroke in rats. *Brain Res* 2012;1445:103-110
36. Baron CA, Kate M, Gioia L, Butcher K, Emery D, Budde M, et al. Reduction of diffusion-weighted imaging contrast of acute ischemic stroke at short diffusion times. *Stroke* 2015;46:2136-2141
37. Yam PS, Dewar D, McCulloch J. Axonal injury caused by focal cerebral ischemia in the rat. *J Neurotrauma* 1998;15:441-450
38. Dewar D, Dawson DA. Changes of cytoskeletal protein immunostaining in myelinated fibre tracts after focal cerebral ischaemia in the rat. *Acta Neuropathol* 1997;93:71-77
39. Nael K, Trouard TP, Lafleur SR, Krupinski EA, Salamon N, Kidwell CS. White matter ischemic changes in hyperacute ischemic stroke: voxel-based analysis using diffusion tensor imaging and MR perfusion. *Stroke* 2015;46:413-418
40. Green HA, Peña A, Price CJ, Warburton EA, Pickard JD, Carpenter TA, et al. Increased anisotropy in acute stroke: a possible explanation. *Stroke* 2002;33:1517-1521
41. Lassen NA. Cerebral blood flow and oxygen consumption in man. *Physiol Rev* 1959;39:183-238
42. Markus HS. Cerebral perfusion and stroke. *J Neurol Neurosurg Psychiatry* 2004;75:353-361
43. Lassen NA, Astrup J. *Ischemic penumbr*a. In: Wood JH, ed. *Cerebral blood flow: physiologic and clinical aspects*. New York, NY: McGraw-Hill, 1987:458-466
44. Plaschke K, Sommer C, Schroeck H, Matejic D, Kiessling M, Martin E, et al. A mouse model of cerebral oligemia: relation to brain histopathology, cerebral blood flow, and energy state. *Exp Brain Res* 2005;162:324-331
45. Takasawa M, Jones PS, Guadagno JV, Christensen S, Fryer TD, Harding S, et al. How reliable is perfusion MR in acute stroke? Validation and determination of the penumbra threshold against quantitative PET. *Stroke* 2008;39:870-877